IEEE Access
Multidisciplinary | Rapid Review | Open Access Journal

Received November 9, 2019, accepted November 28, 2019, date of publication December 3, 2019, date of current version March 10, 2020.

Digital Object Identifier 10.1109/ACCESS.2019.2957383

Efficient Parameters Estimation Methods for Radar Moving Targets Without Searching

XUEPAN ZHANG[1], CHEN YANG[1], QINGQING LIN[1], AND XUEJING ZHANG[2], (Student Member, IEEE)

[1]Qian Xuesen Laboratory of Space Technology, China Academy of Space Technology, Beijing 100094, China
[2]University of Electronic Science and Technology of China, Chengdu 611731, China

Corresponding authors: Qingqing Lin (linqingqing@qxslab.cn) and Xuejing Zhang (xjzhang7@163.com)

This work was supported in part by the National Key Research and Development Program of China under Grant 2017YFB0503300 and Grant 2017YFB0503304, in part by the Youth Talent Promotion Project under Grant 17-JCJQ-QT-046, in part by the Joint Advance Research Program of Aerospace Science and Technology under Grant 6141B06160301, and in part by the National Natural Science Foundation of China (NSFC) under Grant 61701499, Grant 61773383, Grant 41604157, and Grant 11502278.

ABSTRACT Skilled at representing the chirp signal, Radon-Wigner distribution (RWD) plays an important role in parameters estimation for moving targets. By searching for the best time-frequency angle, the conventional RWD estimation method suffers from the tradeoff between the estimation accuracy and computation complexity. In this paper, an efficient RWD estimation method is proposed by exploiting the geometry information in the RWD domain, and extensive parameters searching is replaced by only two parameters computation, then the computation complexity is effectively reduced from O(MN) to O(2N). The proposed efficient RWD method is applied in moving targets velocity estimation, which is emerging issue for smart city. The non-ideal factors in real circumstance are considered, and three robust methods are proposed to improve the estimation accuracy by exploiting the geometry information in the RWD domain further. A clutter suppression RWD (CSRWD) method is proposed to cancel the clutter but preserve the moving target in the RWD domain, and a learned RWD (LRWD) method is proposed to minimize the estimation error caused by measurement error. Then, CSRWD is combined with LRWD to obtain a unified robust RWD (URRWD), which possesses the advantages of CSRWD and LRWD simultaneously. Simulation and real data processing results validate the proposed methods, and lower implementation complexity is proven under the same accuracy assumption. It can be considered as the geometry information opens a window for the searching-based estimation method to make the original bleak searching process suddenly bright. The concept can also be expanded to the other searching-based estimation methods, such as Radon transform, fractional Fourier transform and so on.

INDEX TERMS Radon-Wigner distribution, geometry information, moving targets velocity estimation, SAR, GMTI.

I. INTRODUCTION

Traffic monitoring plays an important role in smart city, and velocity estimation for moving vehicles becomes an emerging issue. Different from the optical observation, Radar can work with almost all weather in day-and-night [1]–[7], which possesses much better advantages. Characterized by wide range, high resolution, cloud penetrating, and remote sensing capability, synthetic aperture radar (SAR) can be used for stationary traffic congestion monitoring; and ground moving targets indication (GMTI) techniques can be used for vehicles velocity estimation and imaging. Thus, SAR-GMTI techniques, has been developed to be an effective and convenient way to realize moving target indication in the well-focused image domain [8], would produce great value in smart city.

As is known, the echoes of moving targets in SAR system are chirp signal, and the velocity can be estimated by the chirp rate. Time-frequency distribution (TFD) is expert in representing the chirp signal [9], which is usually used to estimate the parameters of moving targets. As one of the basic quadratic TFD, the Wigner-Ville distribution (WVD) of a signal is defined as the Fourier transform of the time-dependent

The associate editor coordinating the review of this manuscript and approving it for publication was Liangtian Wan.

autocorrelation function [10]. In the time–frequency plane, the WVD exhibits the highest signal energy concentration for chirp signals [11], then chirp rate can be obtained by measuring the linear slope of the time–frequency spectrum [12]. Naturally, Radon transform (RT), which is usually used for estimating the slope of straight line in the 2-D domain, is operated on the WVD to estimate the chirp rate, i.e. the Radon-Wigner distribution (RWD) [13]. In conventional RWD (CRWD) estimation method, by searching any possible skewed time-frequency angles, the chirp rate is obtained when the RWD reaches the maximum. As is known, both estimation accuracy and computation complexity are determined by the searching step size, i.e. much smaller searching step leads to higher estimation accuracy but huger computation complexity, while much larger searching step leads to lower estimation accuracy with smaller computation complexity. Thus, the searching process of the CRWD estimation method suffers from the tradeoff between estimation accuracy and computation complexity, which largely restricts the development of CRWD in practice, especially in real-time on line system. Some fast estimation methods can reduce the computation complexity by variable searching step sizes, i.e. the large searching step size is used to confirm the parameter interval roughly, and then the small searching step size in this parameter interval is utilized to estimate the parameter accurately.

Different from the existing angles searching methods, an efficient RWD (ERWD) method with low computation complexity and high accuracy is proposed. Instead of time-frequency angles searching, only two time-frequency angles are used to obtain the RWD results, and the corresponding geometry information is used to estimate the chirp rate. So the computation complexity of ERWD is reduced from O(MN) to O(2N).

This paper is organized as follows. In section II, the conventional RWD estimation method is given, contrastively, and the efficient RWD estimation method is proposed by exploiting the geometry information. In section III, the signal model of moving target is SAR-GMTI system is presented, and the application of the proposed ERWD estimation method is given. In section IV, the non-ideal factors in real circumstance are considered, and three robust methods including clutter suppression RWD (CSRWD), measurement error reducing by learned RWD (LRWD) and unified robust RWD (URRWD) are proposed by exploiting the geometry information in the RWD domain further. In section V, simulation and real data process are presented to demonstrate the validity of the proposed methods. And the conclusions are given to summarize the proposed methods in section VI.

II. SIGNAL MODELING

A typical SAR-GMTI geometry model is shown in FIGURE 1. Without loss of generosity, suppose that the target with constant azimuth velocity is located at (x_0, R_0) at the azimuth slow time $\eta = 0$, where radial velocity is not considered since radial velocity can be pre-estimated.

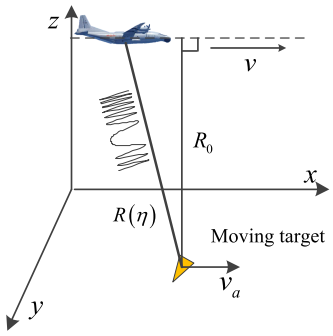

FIGURE 1. Geometry of SAR-GMTI.

According to the geometric relationship, we can get the instantaneous slant-range $R(\eta)$ between the moving target and the SAR platform as follows

$$R(\eta) \approx R_0 + \frac{(v - v_a)^2}{2R_0}(\eta - \eta_0)^2 \tag{1}$$

where v and v_a denote the azimuth velocity of SAR platform and the moving targets, respectively, and η_0 is the radar beam center crossing time of the moving target, expressed as

$$\eta_0 = \frac{x_0}{v - v_a} \tag{2}$$

For a target with constant azimuth velocity, η_0 keeps constant. After range compression and range migration correction, the signal of moving target in azimuth can be written as

$$s(\eta) = \sigma \exp\left(-j\frac{4\pi}{\lambda}\left(R_0 + \frac{(v - v_a)^2}{2R_0}(\eta - \eta_0)^2\right)\right),$$
$$|\eta - \eta_0| \le \frac{T_a}{2} \tag{3}$$

where σ is the scatting coefficient of the moving target, λ is the wavelength of transmitter carrier frequency, and T_a is the synthetic aperture time.

It can be seen from (3) that the signal of moving targets is a chirp signal. In order to realize moving target imaging by azimuth compression, the chirp rate of the moving target should be estimated firstly; and the azimuth velocity of the moving target can also be obtained according to the relationship, which is very important in moving targets recognition. The WVD of $s(\eta)$ can be given as [14]

$$S(\eta, f) = \int_{-\infty}^{+\infty} s\left(\eta + \tau/2\right) s^*\left(\eta - \tau/2\right) \exp\left(-j2\pi f\tau\right) d\tau \tag{4}$$

where f is the Doppler frequency. Substituting (3) into (4), we can obtain the WVD of the moving target as

$$S(\eta, f) = 2T_a\sigma \sin c\left[2\pi T_a\left(\frac{2(v - v_a)^2}{\lambda R_0}(\eta - \eta_0) + f\right)\right] \tag{5}$$

From (5), we can see that the WVD of moving target is sinc-function, and the chirp rate of the moving target can be

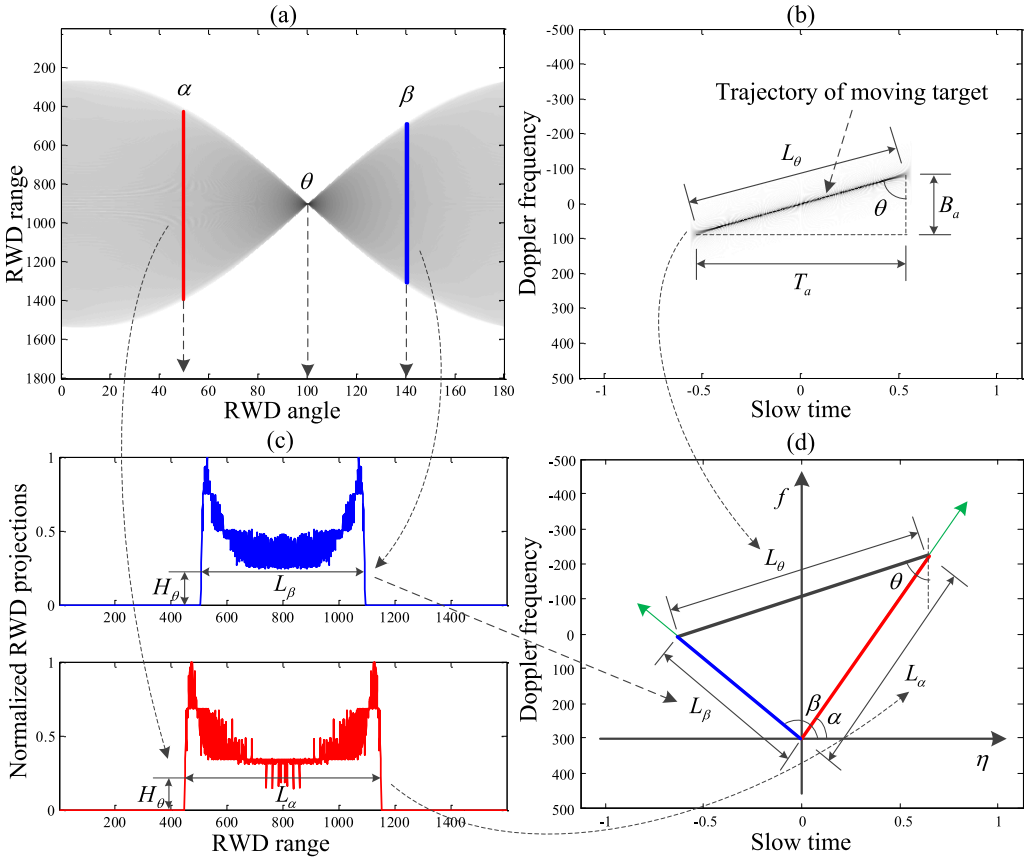

FIGURE 2. Sketch of ERWD. (a) α - and β -RWDs of the chirp signal; (b) WVD of the chirp signal; (c) LNPs of α - and β -RWDs; (d) geometric relationship between LNPs and time-frequency angle.

expressed by the skewed trajectory of moving target in the time-frequency domain as shown in FIGURE 2(b), which is theoretical basis of the RWD estimation. It is obvious to see from (5) that the frequency spectrum of the moving target is linear frequency modulated, and the chirp rate γ_a of the moving target can be expressed as

$$\gamma_a = -\frac{2\left(v - v_a\right)^2}{\lambda R_0} \tag{6}$$

And the chirp bandwidth B_a can be written as

$$B_a = \left|\gamma_a T_a\right| = \frac{2\left(v - v_a\right)^2 T_a}{\lambda R_0} \tag{7}$$

As shown in FIGURE 2(b), the skewed time-frequency angle of moving target is set as θ, and the relationship between θ and γ_a can be obtained by the geometry information as

$$\gamma_a = -\cot\theta \cdot f_{sa} / T_a \tag{8}$$

where f_{sa} is the pulse repetition frequency (PRF) of the system. According to (6) and (8), the azimuth velocity of moving target can also be calculated by

$$\hat{v}_a = v - \sqrt{\lambda R_0 \cot\theta \cdot f_{sa} / 2T_a} \tag{9}$$

The azimuth velocity of moving target is assumed as being lower than that of SAR platform.

So the key problem of estimating the chirp rate and azimuth velocity of moving target turns to estimating the time-frequency angle of moving target.

Skilled at estimating the skewed time-frequency angle, Radon-Wigner distribution (RWD) is mainly considered to estimate the chirp rate in this paper. As the Radon transform of WVD, the RWD of a chirp signal $s(\eta)$ can be expressed as

$$S_R(\rho,\varphi) = \int_{-\infty}^{+\infty}\int_{-\infty}^{+\infty} |S(\eta,f)| \times \delta(\rho - \eta\cos\varphi - f\sin\varphi)\, d\eta df \tag{10}$$

Locating at coordinates of (η, f) in the time-frequency plane, $S(\eta,f)$ denotes the WVD of the chirp signal $s(\eta)$, $|\cdot|$ is the absolute operation, $\delta(\cdot)$ is the impulse function, and $S_R(\rho,\varphi)$ is the Radon transform with range ρ and angle φ.

To estimate the time-frequency angle, the conventional method searches any possible time-frequency angles to estimate that of the chirp signal, and the best matched time-frequency angle can be obtained when the RWD of the chirp signal reaches the maximum, which is the main idea of conventional RWD (CRWD) estimation method.

However, the computation complexity of CRWD as *O(MN)* is mainly caused by the angles and ranges searching, where

M is the number of searched angles, and N is the number of searched ranges. As is known, smaller searching step size of time-frequency angle leads to higher estimation accuracy but huger computation complexity, while larger searching step size brings lower estimation accuracy with smaller computation complexity. Thus, the conventional RWD estimation method suffers from the tradeoff between the estimation accuracy and computation complexity, which would greatly restrict the application of the CRWD in practice.

Focus on these, an efficient RWD (ERWD) estimation method is proposed in the next part, and the computation complexity of ERWD is effectively reduced from *O(MN)* to *O(2N)*.

III. THE PROPOSED EFFICIENT RWD (ERWD) ESTIMATION METHOD

To solve the problems of CRWD as aforementioned, an efficient RWD estimation method without time-frequency angles searching is proposed to calculate the best matched time-frequency angle, and then the chirp rate can be estimated.

The WVD of a chirp signal with time-frequency angle θ is shown in FIGURE 2(b), and the length of the normalized projection (LNP) of the trajectory under a threshold of H_θ is set as L_θ. It should be note that the unit of LNP can be number of the RWD ranges or meters, which is not important since the division is done between LNPs for estimating the parameters in (16) and (17). As shown in FIGURE 2(a), different from all time-frequency angles searching of CRWD, only two angles (α and β) are used to obtain two RWDs (α-RWD and β- RWD) of the chirp signal, as shown in FIGURE 2(c). The LNPs of the α-RWD and β- RWD are measured under threshold of H_θ as L_α and L_β, and threshold selection of H_θ can be set as 0.5 empirically.

The projection nature of Radon transform [15], i.e. Radon transform by an angle of a trajectory can be thought as the projection of the trajectory on the angle, is utilized to obtain the geometrical relationship as shown in FIGURE 2(d).

From FIGURE 2(d), we can get the following geometry information between the LNPs and the time-frequency angles

$$\left|\cos\left(\theta-\left(\frac{\pi}{2}-\alpha\right)\right)\right| = \frac{L_\alpha}{L_\theta} \tag{11}$$

$$\left|\cos\left(\pi-\theta-\left(\beta-\frac{\pi}{2}\right)\right)\right| = \frac{L_\beta}{L_\theta} \tag{12}$$

To calculate the time-frequency angle θ of the chirp signal by (11) and (12), the absolute operation of $|\cdot|$ should be removed according to prior knowledge. The azimuth velocity of ground moving targets can be supposed as being limited in the range of $v_a \in [-50m/s, 50m/s]$, and then θ can be limited in [83.1°, 88.8°] by (9) and the system parameters in TABLE 2. Moreover, the angles (α and β) can be selected as: one angle is less than 83.1°, and the other one is bigger than 88.8°. The absolute operation in (11) and (12) can be removed. And then we can obtain the following results as

$$\sin(\theta+\alpha) = L_\alpha / L_\theta \tag{13}$$

$$-\sin(\theta+\beta) = L_\beta / L_\theta \tag{14}$$

It is assumed that both $\pi > \theta+\alpha > 0$ and $2\pi > \theta+\beta > \pi$ hold simultaneously, and the assumption can be realized by initializing α and β but considering the limited range of θ.

Division is done between (13) and (14) to eliminate the hard measured term of L_θ. By expanding of (13) and (14), one can derive the estimation of $\cot\theta$ as

$$\cot\hat{\theta} = -\frac{L_\beta\cos\alpha + L_\alpha\cos\beta}{L_\alpha\sin\beta + L_\beta\sin\alpha} \tag{15}$$

And the chirp rate of moving target can be calculated by (8) and (15) as

$$\hat{\gamma}_a = \frac{L_\beta\cos\alpha + L_\alpha\cos\beta}{L_\alpha\sin\beta + L_\beta\sin\alpha}\frac{f_{sa}}{T_a} \tag{16}$$

Then the azimuth velocity of moving target can be estimated by (9) and (15) as

$$\hat{v}_a = v - \sqrt{-\frac{L_\beta\cos\alpha + L_\alpha\cos\beta}{L_\alpha\sin\beta + L_\beta\sin\alpha}\frac{\lambda R_0 f_{sa}}{2T_a}} \tag{17}$$

Until now, the time-frequency angle, chirp rate and azimuth velocity are estimated by exploiting the geometry information of two RWD results. By utilizing only two angles to estimate the time-frequency angle, the ERWD estimation method has reduced computation complexity from *O(MN)* to *O(2N)*, which is much more efficient than the CRWD method. Moreover, the estimation accuracy of the CRWD estimation method is restricted by the searching step size as aforementioned, which introduces the tradeoff between the estimation accuracy and computation complexity. It can be seen from (15)∼(17) that the estimation accuracy is affected by the measurement accuracy of the LNPs L_α and L_β, since α and β are known. Thus, compared with the CRWD estimation method, the proposed ERWD estimation method break the limit of the searching step size on estimation accuracy especially, and then the tradeoff mentioned above is also avoided.

Through the analysis above, we can draw the following conclusions: by exploiting the unnoticed geometry information in the RWD domain, the possibly necessary searching process in the estimation method is substituted by calculation, and the computation complexity is reduced from *O(MN)* to *O(2N)*, then the tradeoff between the estimation accuracy and computation complexity is effectively avoided. It can be considered as the geometry information opens a window for the searching-based estimation method to make the original bleak searching process suddenly bright. And the concept can also be used in Radon transform, fractional Fourier transform and so on. Moreover, some new techniques, such as deep learning[16]–[19], can also be used for building the relationship between the geometry information and the parameters.

However, coins have both sides. It can be seen from (15)∼(17) that the estimation of the chirp rate and the azimuth velocity of the moving target is affected by the LNPs, since the other parameters are known. Ideally, the LNPs can be measured accurately, especially in high signal to

noise ratio (SNR) or high signal to clutter ratio (SCR). When the geometry knowledge is not accurately provided, the estimation accuracy would reduce, but some robust methods can be used to improve the estimation performance. In the next section, the robust methods are proposed by exploiting the geometry information further.

IV. THE ROBUST METHODS BY EXPLOITING THE GEOMETRY INFORMATION

According to the estimation by (16) and (17), the estimation accuracy of the ERWD method is mainly dependent on the LNPs. In real circumstance, the clutter would disturb the measurement of LNPs, and the clutter are the echoes of the stationary targets with velocity of zero, which is disadvantageous to moving targets detection and parameters estimation. Furthermore, since the best threshold corresponding to the best estimation of chirp rate is unknown, any selected threshold would bring estimated error, which is called as ''measurement error'' for short. Since the estimation accuracy disturbed mechanisms by clutter and measurement error are different from each other, the robust methods are proposed separately, and then they are unified together to be used in real circumstance with both of clutter and measurement error.

A. CLUTTER SUPPRESSION RWD (CSRWD) ESTIMATION METHOD

In this paper, we focus on the clutter after processing by conventional clutter suppression method, such as space-time adaptive processing (STAP) or displaced phase center antenna (DPCA), so the signal to clutter ratio (SCR) is much higher. A clutter suppression RWD estimation method is proposed to estimate the chirp rate and azimuth velocity of moving target in clutter background. Different from STAP and DPCA, the method cancels the clutter in the RWD domain by two symmetry angles about 90°, and the cancelled results of moving target are exploited to obtain the LNPs for estimating the azimuth velocity.

Located in the same range gate with the moving target, the number of clutter or stationary targets is supposed as N at most. The range compression results of moving target with clutter can be expressed as

$$\begin{aligned} s(\eta) = {} & \sigma_s \exp\left(-j\frac{4\pi}{\lambda}\left(R_0 + \frac{(v-v_a)^2}{2R_0}(\eta-\eta_0)^2\right)\right) \\ & + \sum_{n=1}^{N} \sigma_{cn} \exp\left(-j\frac{4\pi}{\lambda}\left(R_0 + \frac{v^2}{2R_0}(\eta-\eta_n)^2\right)\right), \\ & |\eta-\eta_n| \le \frac{T_a}{2} \end{aligned} \tag{18}$$

where σ_s is the amplitude of moving target, σ_{cn} and η_n denote the amplitude and the radar beam center crossing time of the n th clutter.

To distinguish moving target from clutter in WVD plane, the chirp rate of clutter is corrected to zero by the following matched function

$$s_a(\eta) = \exp\left(j\frac{2\pi v^2\eta^2}{\lambda R_0}\right), \quad |\eta| \le \frac{T_a}{2} \tag{19}$$

Since η_n is unknown, the matching processing is done in the frequency domain, i.e. the Fourier transform (FT) of (18) is multiplied by the FT of (19), then inverse FT (IFT) is done to obtain the results in the slow time domain

$$\begin{aligned} s'(\eta) = {} & \sigma_s \exp\left(-j\frac{4\pi}{\lambda}\left(R_0 + \frac{\gamma_a'\lambda}{4}(\eta-\eta_0)^2\right)\right) \\ & + \sum_{n=1}^{N} \sigma_{cn} \exp\left(-j\frac{4\pi R_0}{\lambda}\right), \quad |\eta-\eta_n| \le \frac{T_a}{2} \end{aligned} \tag{20}$$

where γ_a' is the chirp rate of moving target after correction, which can be written as

$$\gamma_a' = -\frac{2(v-v_a)^2 - 2v^2}{\lambda R_0} \tag{21}$$

It can be seen from (20) that the clutter is corrected to be a single frequency signal, while the moving target is still a chirp signal because of the mismatch. The WVD of (20) can be expressed as

$$\begin{aligned} S(\eta, f) = {} & 2T_a\sigma_s \sin c\left[2\pi T_a\left(\gamma_a'(\eta-\eta_0)+f\right)\right] \\ & + 2T_a \sum_{n=1}^{N} \sigma_{cn} \sin c\left(2\pi T_a f\right) + C \end{aligned} \tag{22}$$

where C is the cross-term of moving target and clutter, and the other two components are auto-terms.

The cross-term lies between the two auto-terms, and it is oscillatory with their frequencies increasing with the increasing distance in the time-frequency domain between the two auto-terms [20]. To estimate the chirp rate in the RWD domain, the cross-term of moving target and clutter should be eliminated firstly. As is known, the cross-term is oscillatory with relatively high frequency, so it can be reduced by the convolution of the WVD with a 2-D ''smoothing kernel'' [20]. In this paper, masked WVD [21] is used to eliminate the cross-term.

As aforementioned, the moving target is still a chirp signal, while the clutter is a single frequency signal. Represented in the WVD domain, the time-frequency angle of moving target is not 90°, while that of clutter is 90°. Based on these characteristics, a clutter suppression RWD estimation method is proposed. Two symmetric angles about 90° (α and β) are used to obtain the RWDs, i.e. the relationship between α and β is $\beta = \pi - \alpha$. The α -RWD of (22) can be expressed as

$$\begin{aligned} & S_R(\rho, \alpha) \\ & = \int_{-B_a/2}^{+B_a/2} \int_{-T_a/2}^{+T_a/2} \left|2T_a\sigma_s \sin c\left[2\pi T_a\left(\gamma_a'(\eta-\eta_0)+f\right)\right]\right| \\ & \quad \cdot \delta(\rho - \eta\cos\alpha - f\sin\alpha)\, d\eta df \\ & \quad + \int_{-B_a/2}^{+B_a/2} \int_{-T_a/2}^{+T_a/2} \left|2T_a \sum_{n=1}^{N} \sigma_{cn} \sin c\left(2\pi T_a f\right)\right| \\ & \quad \cdot \delta(\rho - \eta\cos\alpha - f\sin\alpha)\, d\eta df \end{aligned} \tag{23}$$

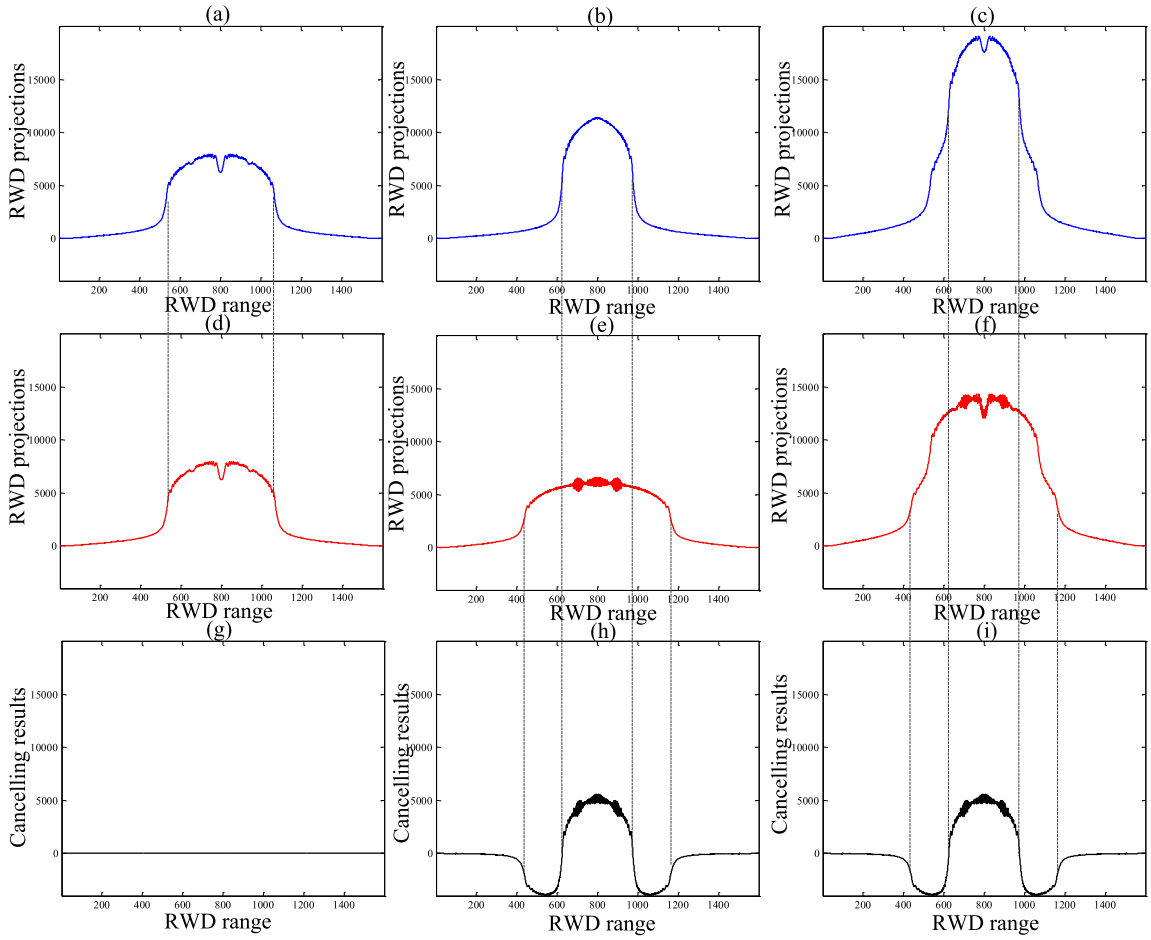

FIGURE 3. The RWD projections and cancelling results of clutter, moving target, and both of clutter and moving target. (a)-(c) is the α -RWD results; (d)-(f) is the β -RWD; (g)-(i) is the cancelling results of α -RWD and β-RWD.

And the β -RWD of (22) can be expressed as

$$\begin{aligned} &S_R(\rho,\beta) \\ &= \int_{-B_a/2}^{+B_a/2}\int_{-T_a/2}^{+T_a/2} \left|2T_a\sigma_s \sin c\left[2\pi T_a\left(\gamma_a'(\eta-\eta_0)+f\right)\right]\right| \\ &\quad \cdot \delta(\rho+\eta\cos\alpha - f\sin\alpha)\,d\eta df \\ &\quad + \int_{-B_a/2}^{+B_a/2}\int_{-T_a/2}^{+T_a/2} \left|2T_a\sum_{n=1}^{N}\sigma_{cn}\sin c\left(2\pi T_a f\right)\right| \\ &\quad \cdot \delta(\rho+\eta\cos\alpha - f\sin\alpha)\,d\eta df \end{aligned} \tag{24}$$

The first terms in (23) and (24) are the RWDs of moving target, while the second terms are the RWDs of clutter. The clutter is assumed as being symmetry about η axis in the synthetic aperture time, then the α -RWD of clutter keep the same as the β -RWD of clutter, while the α -RWD of moving target keep different from the β -RWD of moving target. Realizing these, the α -RWD subtracted by the β -RWD can cancel the clutter and preserve the moving target in the RWD domain. And the cancelling results are shown in FIGURE 3.As shown in FIGURE 3(a) and (d), the α -RWD of clutter almost keeps the same as the β -RWD of it. After the cancelling process, the clutter is suppressed to zero in the RWD domain. But for moving target, the α -RWD results in FIGURE 3(b) and the β -RWD results in FIGURE 3(e) are different from each other, so the moving target is preserved after the cancelling process as shown in FIGURE 3(h). When clutter and moving target are overlapping, the α -RWD and β -RWD of them are shown in FIGURE 3(c) and (f). As shown in FIGURE 3(i), the cancelling result of clutter and moving target almost keep the same as that of only moving target, so the clutter is effectively suppressed.

After clutter suppression in the RWD domain, the geometrical information of the cancelled results are exploited to estimate the chirp rate and azimuth velocity of the moving target. It can be seen from FIGURE 3(h) and (i) that there are protruding and depressed parts in the cancelled results. The results of only moving target in FIGURE 3(b)(e)(h) are analyzed to explain the appearance. Compared with the projection of α -RWD and β -RWD in FIGURE 3(b)(e), the protruding projection of cancelling results is caused by the higher (narrower) projection in FIGURE 3(b), while the depressed projection is caused by the lower (wider) projection in FIGURE 3(e). So the LNP of the protruding part equals to

that of α -RWD, and the LNP of the depressed part equals to that of β -RWD. As shown in FIGURE 3(c) and(f), the α -RWD and β -RWD of moving target and clutter is hybrid, and the LNPs is hard to measure. Considering different properties of clutter and moving target in the RWD domain as aforementioned, the LNPs of the protruding projection and the depressed projection (L_α and L_β) in FIGURE 3(i) can be used to estimate the azimuth velocity.

After chirp rate correction mentioned above, the time-frequency angle of moving target is set as θ', and the relationship between γ_a' and θ' is

$$\hat{\gamma'}_a = -\cot\theta' \cdot f_{sa}/T_a \tag{25}$$

Extensive used for any pair of time-frequency angle, geometry relationship of (15) can also be used for the two symmetric angles about 90° ($\beta = \pi - \alpha$). Then the chirp rate and azimuth velocity of moving target can be estimated by (9) (15) (21) (25) and $\beta = \pi - \alpha$ as

$$\cot\hat{\theta'} = \frac{L_\alpha - L_\beta}{L_\alpha + L_\beta}\cot\alpha \tag{26}$$

$$\hat{\gamma}_a = \frac{L_\beta - L_\alpha}{L_\alpha + L_\beta}\frac{f_{sa}\cot\alpha}{T_a} - \frac{2v^2}{\lambda R_0} \tag{27}$$

$$\hat{v}_a = v - \sqrt{\frac{L_\alpha - L_\beta}{L_\alpha + L_\beta}\frac{\lambda R_0 f_{sa}\cot\alpha}{2T_a} + v^2} \tag{28}$$

So far, the CSRWD has been presented. Two RWDs (α -RWD and β -RWD) of two symmetry angles about 90° ($\beta = \pi - \alpha$) are used to cancel the clutter and preserve the moving target, and the LNPs of protruding and depressed part of the cancelled results are used to estimate the azimuth velocity of moving target. The computation complexity of CSRWD keeps the same as *O(2N)*.

B. MINIMIZING THE MEASUREMENT ERROR BY LEARNED RWD (LRWD)

In this part, a learned RWD estimation method is proposed to minimize the aforementioned measurement error, where the measurement error is the estimated error of azimuth velocity caused by one confirmed threshold. Two angles are used to estimate the time-frequency angle θ of moving target, and extra angle learned by the estimated θ is used to minimize the measurement error.

Since one threshold for measuring the LNPs of α -RWD and β -RWD, the measured error of L_α and L_β is supposed the same as ΔL, and then the estimated error of chirp rate can be written by (16) as follows

$$\begin{aligned}\Delta\hat{\gamma}_a &= \left|\frac{L_\beta\cos\alpha + L_\alpha\cos\beta}{L_\alpha\sin\beta + L_\beta\sin\alpha} - \frac{(L_\beta+\Delta L)\cos\alpha + (L_\alpha+\Delta L)\cos\beta}{(L_\alpha+\Delta L)\sin\beta + (L_\beta+\Delta L)\sin\alpha}\right|\frac{f_{sa}}{T_a} \\ &= \frac{\left|\sin(\alpha-\beta)\,(L_\alpha-L_\beta)\right|\Delta L}{(L_\alpha\sin\beta+L_\beta\sin\alpha)\left((L_\alpha+\Delta L)\sin\beta + (L_\beta+\Delta L)\sin\alpha\right)} \times\frac{f_{sa}}{T_a}\end{aligned} \tag{29}$$

It can be seen from (29) that the $\Delta\hat{\gamma}_a$ is minimized to zero when $L_\alpha = L_\beta$, where $|\sin(\alpha-\beta)| = 0$ is not suitable for the proposed method. According to the geometric relationship, $L_\alpha = L_\beta$ holds when α and β are symmetric about θ, i.e.

$$\beta = 2\theta - \alpha \tag{30}$$

However, θ is unknown and to be estimated. Our strategy to solve this problem is estimating θ for twice: firstly, estimate θ by any pair of α and β, such as symmetry about 90°, and the estimated $\hat{\theta}$ may be with big measurement error; secondly, another RWD angle β' is learned by $\beta' = 2\hat{\theta} - \alpha$, and the estimated error should be minimized by the LNPs of α -RWD and β' -RWD. Through the learning procedure above, the computation complexity of LRWD increases to *O(3N)*.

C. COMPREHENSIVE CONSIDERATION BY UNIFIED ROBUST RWD METHOD (URRWD)

In this part, clutter and measurement error are analyzed together, and a unified robust RWD method is proposed by combining LRWD with CSRWD to be robust to clutter and measurement error.

As is known, two symmetric angles about 90° are used in CSRWD method, while two symmetric angle about θ are used in the LRWD method. But when estimating θ in LRWD method for the first time, the relationship between α and β is no limited, so the two symmetric angles about 90° can be used to cancel the clutter and estimate θ in LRWD method. Another angle is learned by $\beta^* = 2\hat{\theta'} - \alpha$, and its symmetric angle about 90° is $\alpha^* = \pi - \beta^*$ to cancel the clutter, then the measurement error can be minimized by α^* and β^*.

The procedure of the URRWD method is presented as follows:

Step 1: Initialize the transform angle of RWD as α, and the symmetric angle about 90° is $\beta = \pi - \alpha$;

Step 2: Obtain α - RWD and β - RWD of the moving target, and measure the LNPs as L_α and L_β after clutter suppression;

Step 3: Estimate the time-frequency angle θ' of moving target after chirp rate correction by (26), and learn β^* by $\beta^* = 2\hat{\theta'} - \alpha$;

Step 4: Compute the symmetric angle α^* about 90° of β^* by$\alpha^* = \pi - \beta^*$;

Step 5: Obtain β^* - RWD and α^* - RWD of the moving target, and measure the LNPs as L_{β^*} and L_{α^*} after clutter suppression;

Step 6: Utilize the LNPs of L_{α^*} and L_{β^*}, and then the azimuth velocity of moving target can be estimated by combining (17) with (28) as $\hat{v}_a = v - \sqrt{-\frac{\lambda R_0 f_{sa}(L_{\beta^*}\cos\alpha^* + L_{\alpha^*}\cos\beta^*)}{2T_a(L_{\alpha^*}\sin\beta^* + L_{\beta^*}\sin\alpha^*)} + v^2}$.

We can see that the CSRWD method is contained in Step 1, 2, 4, 5 and 6, and the LRWD method is contained in Step 3 and 6. So URRWD can realize the clutter suppression by CSRWD and minimize the measurement error by LRWD, which possesses the advantages of CSRWD and LRWD. By combining LRWD with CSRWD, the computation complexity of URRWD turns to *O(4N)*. Hence, the estimation

TABLE 1. Properties of the RWD estimation methods.

Proposed Methods	Angles of RWDs	Computation complexity	Background
CRWD	All possible	*O(MN)*	Non real-time
ERWD	α , β	*O(2N)*	Ideal
CSRWD	α , β	*O(2N)*	Clutter
URRWD	α , α^* , β , β^*	*O(4N)*	Comprehensive

TABLE 2. System parameters.

Parameters	symbols	values
Carrier frequency/GHz	f_c	8.85
Band width/MHz	B	40
Sampling frequency/MHz	f_{sr}	60
Velocity of the platform/(m/s)	v	120
Pulse repetition frequency/Hz	f_{sa}	1000
Synthetic aperture time/s	T_a	0.639
Nearest slant-range/m	R_n	9000

methods have been presented. Some properties of the methods are summarized briefly in TABLE 1.

Table 1 shows the relationship between α and β to fit for the different background: two symmetry angles about 90° are used to cancel the clutter, and two symmetry angles about θ are used to minimize the measurement error. In the proposed methods, the geometry information and the relationship between the RWD transform angles is exploited efficiently to realize different requirements.

V. EXPERIMENTAL ANALYSIS

Simulation and real data process are given to demonstrate the validity of the proposed methods. And the system parameters are shown in TABLE 2.

A. COMPARISON WITH CRWD METHOD IN COMPUTATION COMPLEXITY AND ESTIMATION ACCURACY

The advantages of the proposed method on computation complexity and estimation accuracy are presented by the comparison with CRWD estimation method. Since tradeoff between computation complexity and estimation accuracy should be considered in CRWD method, two CRWD methods with larger angles searching step of 1° (CRWD1) and smaller angles searching step of 0.1° (CRWD2) are used to compare with the ERWD. Positive and negative azimuth velocities ($v_a \in [-20m/s, 40m/s]$), conclude fast and slow values, are to be estimated to show the effectiveness of wide estimation for azimuth velocities. The estimation results are shown in TABLE 3.

In TABLE 3, the estimated azimuth velocities $\hat{v}_a$ and mean of estimated errors $\Delta\bar{v}_a$ are used to indicate the estimation accuracy, and the estimating time expresses the computation complexity of the methods. From $\hat{v}_a$ and $\Delta\bar{v}_a$, the estimation accuracy of ERWD is much higher than that of CRWD1, but it can equate with that of CRWD2. This is because that the estimation accuracy of CRWD is limited by the searching step size, which can be broken by the proposed method. On the other hand, the computation complexity of ERWD is obviously lower than that of CRWD1 and CRWD2. So the proposed method can realize highly accurate estimation with low computation complexity, which is very suitable for the real-time systems. Furthermore, the standard deviation of estimated error σ_v is used to express the wide application property for different azimuth velocities. It can be seen that the wide estimation property of ERWD is the best, i.e. the proposed method is more accurate than CRWD in estimating azimuth velocities.

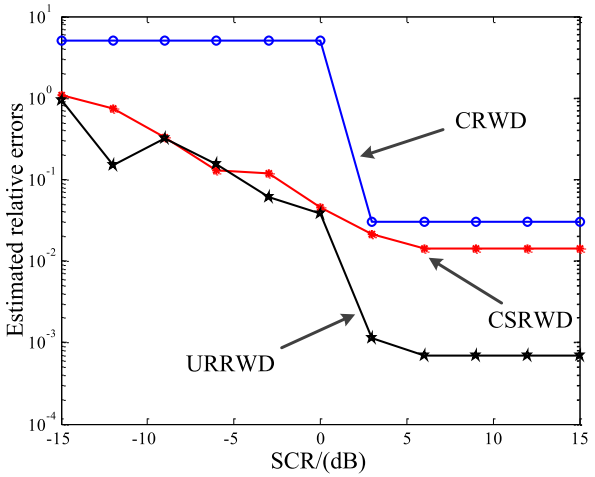

FIGURE 4. Comparisons in clutter background.

B. CLUTTER BACKGROUND AND MEASUREMENT ERROR ANALYSIS

Clutter background and measurement error are analyzed in this part. In clutter background, the application mechanism of CRWD is different from that of the proposed methods: CRWD utilizes time-frequency angles searching to accumulate the energy of moving target; while the proposed robust methods make use of the geometry relationship between two symmetry RWDs to cancel the clutter and preserve the moving target in the RWD domain. In addition, measurement error should be minimized in clutter background. Under different output SCR after range compression, the estimation accuracy of CRWD, CSRWD and URRWD is compared in FIGURE 4.

It is obviously that the estimated relative errors of CSRWD and URRWD are much lower than that of CRWD in all SCR, illustrating that the clutter cancelling (in CSRWD and URRWD methods) is much more effective in improving the SCR than angles searching (in CRWD method). In addition, it can be seen from FIGURE 4 that the stable estimation accuracy of CSRWD and URRWD is higher than that of

TABLE 3. Estimation results by ERWD and CRWD methods.

v_a (m/s)		-20.0000	-8.0000	4.0000	16.0000	28.0000	40.0000	$\Delta\overline{v}_a$	σ_v
$\hat{v}_a$ (m/s)	CRWD1	-19.3500	-9.9404	5.2679	16.4345	28.8135	43.0277	-0.3149	1.6920
	CRWD2	-20.2658	-7.9969	3.6737	15.8511	28.1578	39.9910	-0.0513	0.1500
	ERWD	-19.9970	-7.9911	4.0166	16.0220	28.0529	40.0105	0.0765	0.0689
Estimating time(s)	CRWD1	3.6258	3.5564	3.5484	3.6070	3.6337	3.5987	--	--
	CRWD2	34.9542	34.2901	34.5248	34.1640	34.8808	34.6069	--	--
	ERWD	0.1053	0.1054	0.1123	0.1062	0.1032	0.1072	--	--

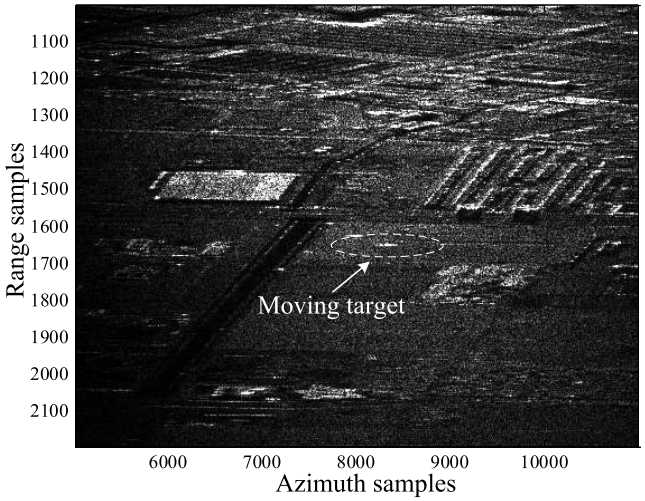

FIGURE 5. The imaging result of moving target using chirp rate of scene.

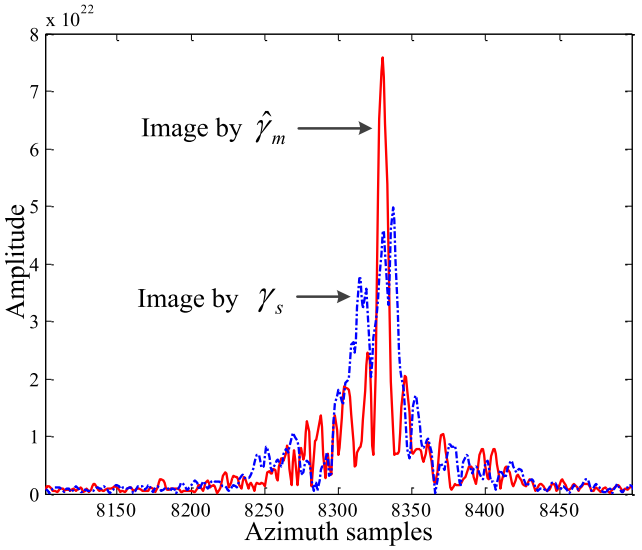

FIGURE 6. The imaging result of moving target using the estimated chirp rate by URRWD.

CRWD. The results demonstrate that the proposed methods can break through the estimation accuracy restriction by the time-frequency angles searching step. This is because the estimation accuracy of the proposed methods is limited by time-frequency resolution as aforementioned, which is independent on time-frequency angles searching step. Furthermore, the estimation accuracy of URRWD is higher than that of CSRWD. In URRWD method, not only the clutter is cancelled, but also the measurement error is minimized. So URRWD possesses much more competitive advantage than CSRWD.

C. REAL DATA EXPERIMENTS

Real data is processed to demonstrate the effectiveness of the proposed method. The real data is recorded by an airborne X-band radar system, and the system parameters are shown in TABLE 2. The range-Doppler imaging algorithm is used to image the scene and moving target. After azimuth compression by chirp rate of static scene γ_s, the imaging result is shown in FIGURE 5. We can see that the scene is well-focused, while the moving target is defocused, and the azimuth compression result of moving target is shown in FIGURE 6.

The reason is that the azimuth velocity of moving target leads to a different chirp rate from that of scene. Then the matched function of azimuth compression is mismatched for the moving target. So if we want to get the well-focused image of moving target, the chirp rate or the azimuth velocity of the moving target should be estimated. URRWD is used to estimate the chirp rate of the moving target. After the estimating steps of URRWD, the chirp rate of moving target is estimated as $\hat{\gamma}_m = -83.0412 Hz/s$, and the azimuth velocity can be calculated as $1.4509 m/s$. The moving target is refocused by $\hat{\gamma}_m$, and the azimuth compression result is shown in FIGURE 6.

It can be seen that the moving target is well-focused, demonstrating the validity of the estimated chirp rate and azimuth velocity of moving target by URRWD. In addition, the advantage of URRWD in lower computation complexity is more competitive than CRWD in real-time system.

VI. CONCLUSION

By exploiting the unnoticed geometry information in the RWD domain, an efficient and accurate RWD estimation method is proposed to estimate the chirp rate and azimuth

velocity of moving target. Instead of searching for the time-frequency angles in conventional RWD estimation method, the geometry information of the two RWDs by two angles are used to compute the time-frequency angle of the moving target. And the computation complexity of the proposed method is effectively reduced from *O(MN)*to *O(2N)*.

Clutter background and measurement error are considered, and the corresponding robust methods (CSRWD and LRWD) are proposed by utilizing the geometry relationships further. Since the geometry of clutter and moving target in the RWD domain are different, two RWDs of two symmetry angles about 90° are used to cancel the clutter but preserve the moving target. In addition, two symmetric angles about the time-frequency angle of moving target are utilized to minimize the estimated error caused by threshold selection. And LRWD and CSRWD are unified together as URRWD to be used in the real circumstance with clutter and measurement error. Simulation and real data process show that the proposed methods can estimate the azimuth velocity of moving target in high accuracy with lower computation complexity. The advantage of the proposed methods in lower computation complexity is more competitive than CRWD in real-time systems.

Utilizing the geometry information, the computation complexity is reduced effectively. It can be considered as the geometry information opens a window for the searching-based estimation method to make the original bleak searching process suddenly bright. And the concept can also be used in Radon transform, fractional Fourier transform and so on. In the future work, deep learning technique and other estimation methods [22-27] should be considered to improve the estimation accuracy further.

ACKNOWLEDGMENT

The authors would like to thank the anonymous reviewers for their valuable and useful comments and suggestions which helped to improve the article.

REFERENCES

[1] C. H. Gierull, I. Sikaneta, and D. Cerutti-Maori, "Two-step detector for RADARSAT-2's experimental GMTI mode," *IEEE Trans. Geosci. Remote Sens.*, vol. 51, no. 1, pp. 436–454, Jan. 2013.
[2] F. Wen, Z. Zhang, G. Zhang, Y. Zhang, X. Wang, and X. Zhang, "A tensor-based covariance differencing method for direction estimation in bistatic MIMO radar with unknown spatial colored noise," *IEEE Access*, vol. 5, pp. 18451–18458, 2017.
[3] F. Wen, J. Shi, and Z. Zhang, "Direction finding for bistatic MIMO radar with unknown spatially colored noise," *Circuits, Syst., Signal Process.*, pp. 1–13, 2020, doi: 10.1007/s00034-019-01260-5.
[4] F. Wen, Z. Zhang, and G. Zhang, "Joint DOD and DOA estimation for bistatic MIMO radar: A covariance trilinear decomposition perspective," *IEEE Access*, vol. 7, pp. 53273–53283, 2019.
[5] F. Wen, C. Mao, and G. Zhang, "Direction finding in MIMO radar with large antenna arrays and nonorthogonal waveforms," *Digital Signal Process.*, vol. 94, pp. 75–83, Nov. 2019.
[6] X. Li, Z. Sun, G. Cui, L. Kong, X. Yang, and W. Yi, "Computationally efficient coherent detection and parameter estimation algorithm for maneuvering target," *Signal Process.*, vol. 155, pp. 130–142, Feb. 2019.
[7] L. Wan, G. Han, D. Zhang, A. Li, and N. Feng, "Distributed DOA estimation for arbitrary topology structure of mobile wireless sensor network using cognitive radio," *Wireless Pers. Commun.*, vol. 93, no. 2, pp. 431–445, Feb. 2017.
[8] M. D. Graziano, M. D'Errico, and G. Rufino, "Ship heading and velocity analysis by wake detection in SAR images," *Acta Astronautica*, 2016, pp. 72–82, Nov./Dec. 128.
[9] J.-W. Park and J.-S. Won, "An efficient method of Doppler parameter estimation in the time–frequency domain for a moving object from TerraSAR-X data," *IEEE Trans. Geosci. Remote Sens.*, vol. 49, no. 12, pp. 4771–4787, Dec. 2011.
[10] L. Cohen, "Time-frequency distributions-a review," *Proc. IEEE*, vol. 77, no. 7, pp. 941–981, Jul. 1989.
[11] M. Kirscht, "Detection and imaging of arbitrarily moving targets with single-channel SAR," *IEE Proc.-Radar, Sonar Navigat.*, vol. 150, no. 1, pp. 7–11, 2003.
[12] F. Sattar and G. Salomonsson, "The use of a filter bank and the Wigner-Ville distribution for time-frequency representation," *IEEE Trans. Signal Process.*, vol. 47, no. 6, pp. 1776–1783, Jun. 1999.
[13] J. C. Wood and D. T. Barry, "Linear signal synthesis using the Radon-Wigner transform," *IEEE Trans. Signal Process.*, vol. 42, no. 8, pp. 2105–2111, Aug. 1994.
[14] G. C. Gaunaurd and H. C. Strifors, "Signal analysis by means of time-frequency (Wigner-type) distributions-applications to sonar and radar echoes," *Proc. IEEE*, vol. 84, no. 9, pp. 1231–1248, Sep. 1996.
[15] Z. Zalevsky and D. Mendlovic, "Fractional radon transform: Definition," *Appl. Opt.*, vol. 35, no. 23, pp. 4628–4631, 1996.
[16] H. Huang, J. Yang, H. Huang, Y. Song, and G. Gui, "Deep learning for super-resolution channel estimation and doa estimation based massive MIMO system," *IEEE Trans. Veh. Technol.*, vol. 67, no. 9, pp. 8549–8560, Sep. 2018.
[17] J. Wang, Y. Ding, S. Bian, Y. Peng, M. Liu, and G. Gui, "UL-CSI data driven deep learning for predicting DL-CSI in cellular FDD systems," *IEEE Access*, vol. 7, pp. 96105–96112, 2019.
[18] Y. Wang, M. Liu, J. Yang, and G. Gui, "Data-driven deep learning for automatic modulation recognition in cognitive radios," *IEEE Trans. Veh. Technol.*, vol. 68, no. 4, pp. 4074–4077, Apr. 2019.
[19] G. Gui, H. Huang, Y. Song, and H. Sari, "Deep learning for an effective nonorthogonal multiple access scheme," *IEEE Trans. Veh. Technol.*, vol. 67, no. 9, pp. 8440–8450, Sep. 2018.
[20] G. R. Arce and S. R. Hasan, "Elimination of interference terms of the discrete Wigner distribution using nonlinear filtering," *IEEE Trans. Signal Process.*, vol. 48, no. 8, pp. 2321–2331, Aug. 2000.
[21] L. Zuo, M. Li, X. Zhang, Y. Wang, and Y. Wu, "An efficient method for detecting slow-moving weak targets in sea clutter based on time–frequency iteration decomposition," *IEEE Trans. Geosci. Remote Sens.*, vol. 51, no. 6, pp. 3659–3672, Jun. 2013.
[22] X. Zhang, Z. He, B. Liao, Y. Yang, J. Zhang, and X. Zhang, "Flexible array response control via oblique projection," *IEEE Trans. Signal Process.*, vol. 67, no. 12, pp. 3126–3139, Jun. 2019.
[23] C. Wang, Z. Qiu, M. Xu, and Y. Li, "Mixed nonprobabilistic reliability-based optimization method for heat transfer system with fuzzy and interval parameters," *IEEE Trans. Rel.*, vol. 66, no. 3, pp. 630–640, Sep. 2017.
[24] C. Yang, Z. Lu, and Z. Yang, "Robust optimal sensor placement for uncertain structures with interval parameters," *IEEE Sensors J.*, vol. 18, no. 5, pp. 2031–2041, Mar. 2018.
[25] H. Wang, L. Wan, M. Dong, K. Ota, and X. Wang, "Assistant vehicle localization based on three collaborative base stations via SBL-based robust DOA estimation," *IEEE Internet Things J.*, vol. 6, no. 3, pp. 5766–5777, Jun. 2019.
[26] X. Wang, L. Wan, M. Huang, C. Shen, and K. Zhang, "Polarization channel estimation for circular and non-circular signals in massive MIMO systems," *IEEE J. Sel. Topics Signal Process.*, vol. 13, no. 5, pp. 1001–1016, Sep. 2019.
[27] L. Wan, X. Kong, and F. Xia, "Joint range-Doppler-angle estimation for intelligent tracking of moving aerial targets," *IEEE Internet Things J.*, vol. 5, no. 3, pp. 1625–1636, Jun. 2018.

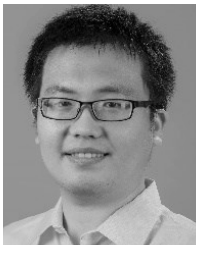

XUEPAN ZHANG was born in Hebei, China. He received the B.S. and Ph.D. degrees in electrical engineering from the National Laboratory of Radar Signal Processing, Xidian University, Xi'an, China, in 2010 and 2015, respectively. He is currently a Principal Investigator with the Qian Xuesen Laboratory of Space Technology, Beijing, China. His current research interests include synthetic aperture radar, ground moving target indication, and deep learning.

CHEN YANG received the bachelor's, master's, and Ph.D. degrees in engineering mechanics and solid mechanics from Beihang University (BUAA), Beijing, China, in 2010, 2013, and 2018, respectively. He is currently an Associate Professor with the Qian Xuesen Laboratory of Space Technology, China Academy of Space Technology. He has published over 40 research articles in the journals, particularly in the area of intelligent optimization algorithms and its applications. His research interests include optimization theory, structural health monitoring, optimal sensor placement, structural dynamics, and thermal control.

QINGQING LIN was born in 1987. She received the B.S. and Ph.D. degrees in information and communication engineering from the Harbin Engineering University, Harbin, China, in 2009 and 2013, respectively. Since 2013, she has been a Research Assistant with the Qian Xuesen Laboratory of Space Technology, China Academy of Space Technology, Beijing, China. Her research interests include array signal processing and wireless sensor networks.

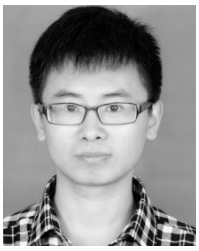

XUEJING ZHANG (S'17) was born in Hebei, China. He received the B.S. degree in electrical engineering from Huaqiao University, Xiamen, China, in 2011, and the M.S. degree in signal and information processing from Xidian University, Xi'an, China, in 2014. He is currently pursuing the Ph.D. degree in signal and information processing with the School of Information and Communication Engineering, University of Electronic Science and Technology of China (UESTC), Chengdu, China. Since November 2017, he has been a Visiting Student at the University of Delaware, Newark, DE, USA. His research interests include array signal processing and wireless communications.